

LINAC INTEGRATED SCHEME USING RF ENERGY STORAGE AND COMPRESSION

A.V. Smirnov, Russian Research Center "Kurchatov Institute", Moscow, 123182, Russia

Proposed earlier the conception of a compact rf-linac without an external rf-energy source is analysed here numerically. Under certain conditions an unbunched low voltage electron beam can be accelerated during a short ns pulse by using of rf-energy stored in an external cavity for a relatively long time of self-excited oscillation induced by the same beam in the same special accelerating/oscillating linac structure. Non-steady acceleration is considered in terms of optimal time delays, energy gain and spectra.

I. INTRODUCTION

In the previous paper [1] we showed the feasibility of a low energy linac combining rf-generation and acceleration processes at the same injected beam energy. It is based on use of rf-compression technique developed for high energy linear colliders. Since the RF energy commutation may be one or two orders faster than the electric high voltage energy commutation (conventional modulator), combining the structure proposed and RF energy compression system can give high levels of the average beam power (10-100kW). The linac facility would have considerably reduced weight and sizes as compared to similar industrial linacs. The power supply required is in 40-120 kV range dc source, and an estimated overall wall plug efficiency is about a one percent.

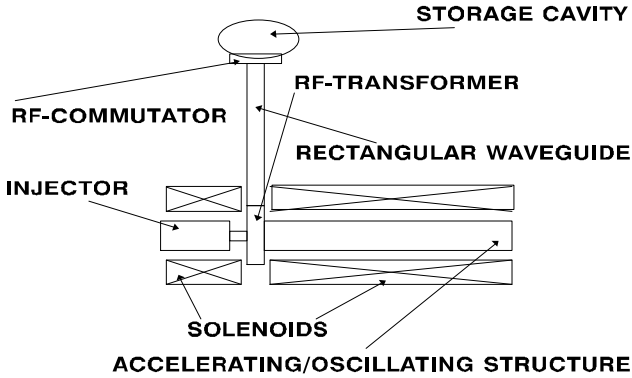


Figure 1. The integrated linac scheme for the case of the acceleration by the forward wave. The rf commutator contains an auxiliary modulator (it is not shown) to control the external Q_e of the storage cavity.

II. PRELIMINARY ASSUMPTIONS AND INPUT CONDITIONS

We are considering here only one of two integrated linac schemes [1]. It utilizes acceleration by the forward wave and oscillation of the backward wave. The schematic layout is shown in the Figure 1.

Concerning the processes of rf generation and compression discussed earlier [1-3], here we consider only more accurately the efficiency of energy transfer from the structure to cavity and back. It is advantageous to use a periodic regime when the cavity is not empty before energy storage. Apart from [4], we assume external rf energy source does not exist during the time interval for energy transfer from the cavity to the accelerating structure. For this case the storage efficiency can be calculated by imposing periodicity condition:

$$\eta_{st} = \frac{2\chi_g}{\mu(1+\chi_g)} \left[1 - \frac{1-e^{-\delta}}{1-e^{-(\mu+\delta)}} e^{-\mu} \right]^2, \quad (1)$$

where $\delta = \pi t_f f_0 (1 + \chi_u) / Q_0$, $\mu = \pi t_g f_0 (1 + \chi_g) / Q_0$, t_g is the time duration of the RF power storage in the external cavity, f_0 is the operating frequency, t_f is the section filling time, χ_g is the coupling factor during the rf-energy generation and storage, and χ_u is the coupling factor during the time interval t_u , during that the stored energy is coupled out of the storage cavity with factor Q_0 . The maximum value of η_{st} approaches 1 instead of 0.815 and at the limit of $\chi_u \rightarrow \infty$ we obtain usual expression. It can be seen from (1), that the optimum value of μ is 0.9 (when $\delta = 1.26$) instead of usual 1.262.

For a constant impedance structure and a storage cavity with two RF-ports the efficiency η_0 of energy transfer from the cavity to structure is calculated by P.B. Wilson [5]. For our case the corresponding efficiency is:

$$\eta_0 = 2\delta \frac{\chi_\mu}{1 + \chi_\mu} \left(\frac{e^{-\delta} - e^{-\alpha L_3}}{\delta - \alpha L_3} \right)^2, \quad (2)$$

where α is the attenuation constant. For a constant gradient structure one can obtain:

$$\eta_0 = 2\delta \frac{\chi_u}{1 + \chi_u} \frac{1 - e^{-2\tau}}{2\tau} \left(\frac{1 - e^{-\delta}}{\delta} \right)^2. \quad (3)$$

Here τ is the attenuation parameter, and to maximise η_0 we should provide $\delta \approx 1.26$.

Time-dependent calculations were undertaken to confirm and specify the analytical estimations (see the first column of the Table 2 in ref.[1]). The RF energy, entering into the section from the storage cavity, and the total charge of the input pulse train were 1.34 J and 83 nC respectively. A constant impedance subsection L_3 was assumed.

The modified code [6] used takes into account non-steady beam loading, accelerating wave propagation in the tapered section and longitudinal space charge effect. As an example we used the optimised DLWG section parameters presented in Fig. 2.

Accurate optimisation of these parameters depends on the current pulse and RF power pulse shapes as well as time delay t_d between them. To simulate real pulse shapes we have used non-ideal profiles for the incident RF pulse (see Fig. 3) and the input current pulse (see Fig. 4, curve 1).

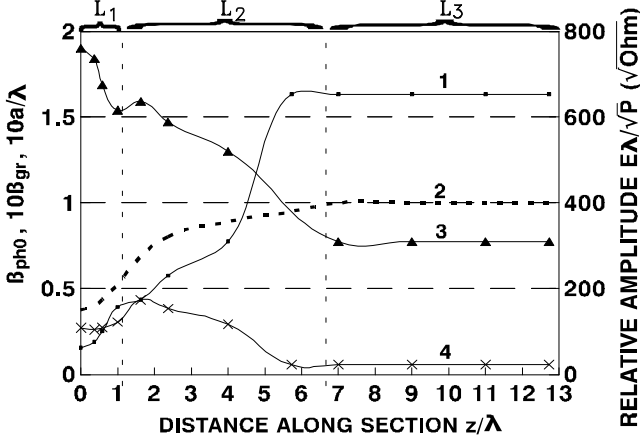


Figure 2. The parameters of the optimised DLWG tapered structure plotted along the section: relative accelerating field amplitude (curve 1), relative phase velocity for the fundamental harmonic β_{ph0} (curve 2), iris relative radius a/λ (curve 3) and relative group velocity (4)

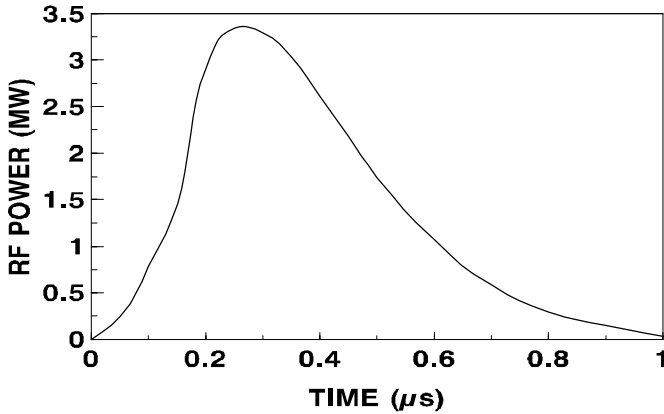


Figure 3. Input RF power pulse profile used in simulations. RF energy is equal to 1.34 J.

III. SIMULATION RESULTS

Under the conditions given above we have found geometrical and RF parameters for the linac section (see Fig. 2) that provide close to the maximum accelerated beam energy (see Fig. 4) and capture coefficient at optimal time delay $t_d \approx 0.6 \mu s$. Note, that the undesirable phase shifting cells were avoided at this optimisation.

It is seen from Fig. 5, that the beam capture is equal to its maximum at $t_d \approx 0.48 \mu s$ and the full width of the energy spectrum at half maximum (FWHM) is equal to the local minimum value with both time delays. Energy spectra calculated for the total accelerated pulse train at these values of time delay are presented in Figs. 6a,b.

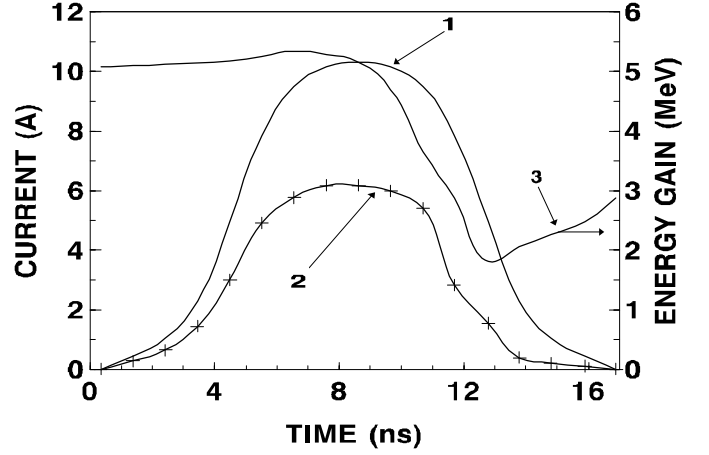


Figure 4. Input current pulse profile (curve 1) used in simulations. Injected pulse charge is equal to 83 nC. Output current pulse profile (curve 2) and energy gain versus time (curve 3) are calculated for the time delay $t_d = 0.58 \mu s$ and RF energy 1.34 J. Accelerated pulse charge is equal to 47 nC.

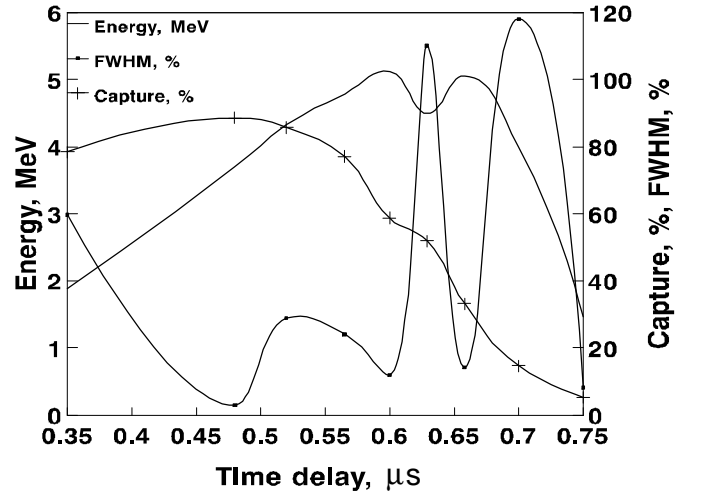


Figure 5. Beam capture coefficient, energy gain and energy spectrum FWHM for the accelerated pulse train as a function of the time delay between the injected current pulse and the RF pulse.

A non-steady beam loading effect is demonstrated in Fig. 4 (curves 2,3) for close to optimal parameters of the section and time delay. We see, that the energy averaged over the bunch is a non-monotonous function of the bunch number. It is caused by a combined effect of the sharp form of the incident RF-pulse and non-ideal injected current profile.

It was found in simulations [6], that the total energy spread is narrower for asymmetric input pulse current profile having long leading edge and short trailing edge if the section filling time and pulse length are comparable.

The simulations presented above imply pulsed injection from ns electron gun. However, it would be interesting to consider the case of continuous beam injection. Calculation results for the input dc $I=9$ A beam are presented in Fig. 7.

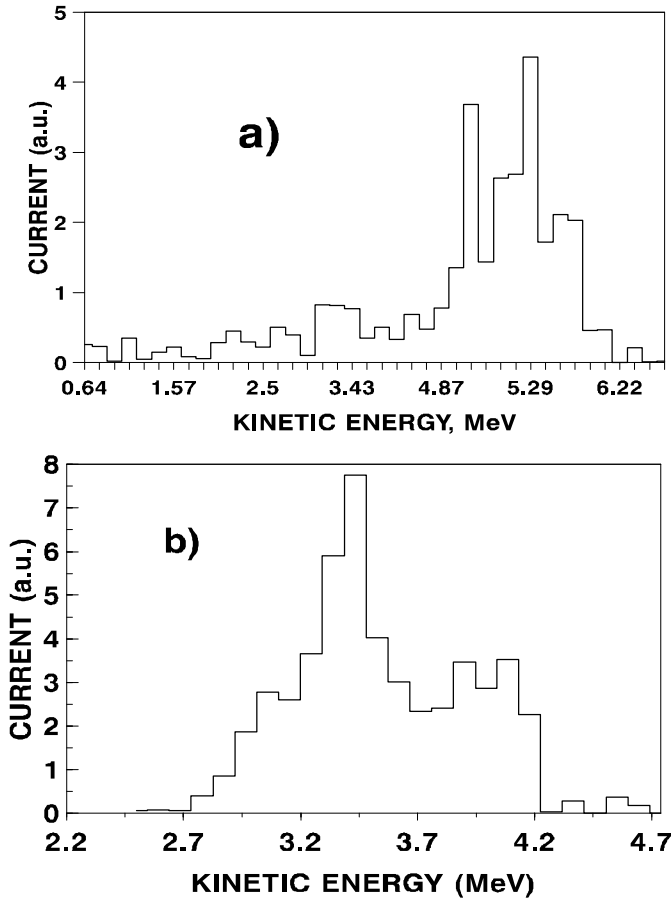


Figure 6. Energy spectra for the accelerated pulse train for two different time delays: $t_d = 0.6 \mu s$ (a) and $t_d = 0.5 \mu s$ (b).

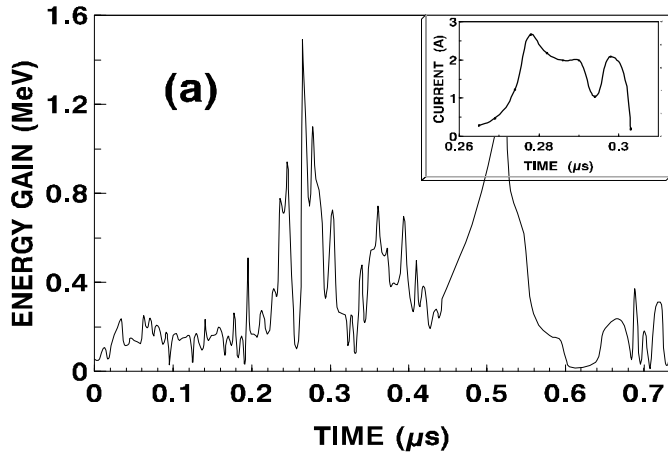


Figure 7.a. Electron beam energy gain and current versus time for RF energy 1.34 J. The inset shows the accelerated current pulse shape corresponding to the maximum energy. RF power pulse shape and duration are the same that depicted in Fig. 3.

The reason of low energy gain (see Fig. 7,a) is a competition between the processes of trapping into acceleration - on the one hand and oscillation (radiation) of the -1 and

fundamental space harmonics - on the other. In accordance with the simulation results Fig. 7,b it is necessary to treble the peak RF power (and, consequently, RF energy stored) to achieve the same peak energy gain.

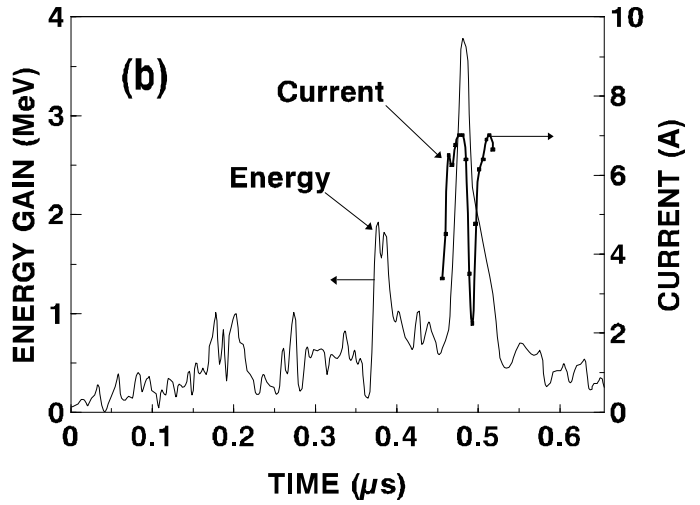


Figure 7.b. Electron beam energy gain and current versus time for RF energy 4 J. RF power pulse shape and duration are the same that depicted in Fig. 3.

IV. SUMMARY

The most effective performance requires the electron gun turning off during the structure filling in by rf-energy and optimization of the time delay between rf-switching and electron gun turning on. In this case analytical estimations are in agreement with simulation results.

V. REFERENCES

- [1] A.V. Smirnov, V.N. Smirnov. A Conceptual Design of a One-Section Linac Using RF-Energy Compression. Proc of the 4-th European Particle Accelerator Conf. EPAC-94, p. 774
- [2] A.V. Smirnov, V.N. Smirnov, Beam Self-Excited Oscillation in Linac Buncher Section. Nucl. Instrum. and Meth. A349 (1994) 614
- [3] A.V. Smirnov, V.N. Smirnov, K.E. Sokolov. An Operative Measurement of RF Parameters for Slow-Wave Systems, Proc. EPAC-94, V. 3, p. 1995.
- [4] Z.D. Farkas. RF Energy Compressor. IEEE MTT-S Int. Microwave Symposium Digest. New York, (1980) p.84-86
- [5] D.L. Birx, Z.D. Farkas, P.B. Wilson. A Look at Energy Compression as an Assist for High Power RF Production. AIP Conf. Proc. 153, Vol.2, New York, 1987.
- [6] A.V. Smirnov. Numerical Investigation of Non Steady Dynamics Effects of Intense Beam in Linac Transition Regime. Proc. of the 11-th All-Union Conf. on Charged Particles Accelerators. Proc. of the 11-th All-Union Conf. on Charged Particles Accelerators, (Dubna, JINR, USSR, 1989), Vol.1, 488